An Autonomous Drone System for Scanning an Electric Field Using Visual Feedback

1st Artur Zawadzki
ABB Corporate Technology Center
Krakow, Poland
artur.zawadzki@pl.abb.com

2rd Marcin Firla
ABB Corporate Technology Center
Krakow, Poland
marcin.firla@pl.abb.com

3nd Piotr Ryba
ABB Corporate Technology Center
Krakow, Poland

2021 IEEE 26th International Conference on Emerging Technologies and Factory Automation (ETFA) | 978-1-7281-2989-1/21/$31.00 ©2021 IEEE | DOI: 10.1109/ETFA45728.2021.9613381

***Abstract*—Measuring of the electric field strength in the proximity of high-voltage devices, even several hundred thousand volts, both in the case of AC and DC current, is a challenging and dangerous task. Furthermore, in many cases the measurement seems to be even impossible to carry out. During gauging the electric field it is necessary to provide insulation between the sensor and the ground which involves the need to maintain a large distance from the grounding point. In light of the problems described, the use of drones for measurements could be a good solution. This paper describes selected aspects of a complex system ready to perform automatic mapping of the electric field. It includes the description of AC and DC sensors, proof of concept of electric field mapping with a manually operated drone, and the proposed automatic control system. The paper tackles experiment aspects by presenting various tries executed for system development as well as full case study showcasing a complete solution. Finally, the paper presents a method of electric field measurement carried out by the proposed fully automatic system based on vision feedback that uses the scanning trajectories to control the drone. As a result, the proposed method enables measuring the distribution of the electric field in the three-dimensional space that provides information not available otherwise. Therefore that could be exploited to e.g. the insulation damage detection. The main advantage of the proposed system is the fully autonomous process of scanning that could be employed in widely-understood devices diagnostic.**

***Index Terms*—Drone, Electric field mapping, Autonomous control, AC/DC field sensor, Image processing**

I. Introduction

High-voltage equipment, for example switchgears, high-voltage direct current (HVDC) stations and current distribution components with a voltage ranging from several thousand volts to several hundred thousand volts, must be operated with sufficiently large insulation distances. As a result, any measurement of electrical or non-electrical values requires specialized equipment and very demanding safety procedures [1]. It is obvious that such sensing make sense mainly when the devices are in operation. Measurement difficulties may provide a rough results of, for example, electric field distribution. It is usually assumed that the numerical model of the field distribution may be so precise, that it is only necessary to selectively verify it. Meanwhile, the field distribution over time is not constant and may change its form depending on the device state, potential damage, insulation condition or shielding degradation. This type of damage may not be detectable by visual inspection.

Using drones for different measurements have become quite popular in last years [2] [3]. The main advantage in this case is the relatively easy access to elements of the installation, which are difficult to achieve using traditional methods. The undoubted advantage of drones in case of electric field measurement is not only radio-controlled and independent power supply, but also that the drones are not grounded during the flight. This means that the measurement becomes much safer and incomparably easier.

However, drones require control. Currently, manual control by a human operator is most often used, and flight aids, such as vision systems, are used to support manual control (e.g. First-Person View cameras). Automatic flight systems are also used, usually based on complex and therefore expensive systems [4]. It is also possible to use vision systems for fully automatic flight along a preset trajectory [5]. The common problem is to accurately determine the position of the drone in the three-dimensional space [6]. Apart from the systems based on LiDAR [7], interesting approach used are SLAM techniques [8] [9]. However, they are usually characterized by limited accuracy, not entirely sufficient for precise and repeatable space scanning (e.g. because of uniform texture of environment). On the other hand, GPS-based systems do not function in confined spaces, which is often the case in DC switchgears or HVDC stations placed in halls. Sometimes RTK (Real-Time Kinematic) systems are used as a method of increasing accuracy of GPS. It is based on differential GPS measurements, taking into account known reference point locations, which are then paired with the drone's measurements [10]. That system increases position accuracy to few centimeters range but RTK is still limited to operation in the open air area. Therefore, a different approach for accurate indoor drone positioning is needed.

Drones are broadly used for various types of surveillance e.g. inspection of transmission lines, but that is performed mostly outdoor and using camera or thermal scan to obtain pictures of facilities [11] [12]. On the other hand, the indoor autonomous flights are also active research area e.g. due to Indoor Autonomy Challenge that is organized together with International Micro Air Vehicle Conference [13].

The novelty proposed in this paper covers the system designed with a purpose of operating in area dangerous for humans. This paper proposes to measure directly electric field

in proximity of operating HV devices. That is examined with AC and DC custom sensors that are also described in the paper. Another contribution is the system design based on ArUco markers that gives a possibility for periodic inspection of the selected indoor area. The main focus of the paper is a unique approach for indoor inspection performed with drone. While all the elements are known in the state of the art of each technical field, the combination of all is novel.

The paper is organized as follows. In Section II the constructed electric field sensors are described. In Section III number of tests conducted during the system development are presented. Section IV describes vision-based approach for drone positioning that uses ArUco codes. In Section V control strategy is described. Finally, the case study with fully autonomous flight is described in Section VI. At the end in Section VII there is a short summary with future outlook.

II. Electric field sensors

There are several, know methods of DC electric field measurement. The most popular methodology is based on electro-optical Pockels effect and field mill sensor construction where mechanically modulated DC field generates AC current [14].

It is also possible to find other methodology based on e.g. MEMS [15], but in most cases these are only research prototypes, developed on universities, which are complex and give not so good results in comparison to well-known solutions.

To be able to create a compact sensor for a wide measurement range, the field mill sensor architecture was selected. It is based on three components: the modulator, the detector, and the amplifier. The modulator can be realized in many different ways. The most common practice is based on a propeller shape which is rotating with constant speed driven by electric motor. The propeller located in the DC electric field modulates this field and creates a sinusoidal signal. The generated AC electric field affects the detector and induces a current which is converted by amplifier. This signal can be measured and processed to obtain the information about the electric field strength. The field mill is able to determine the field strength by measuring capacitance based on induced electric charge.

The most common architecture of the field mill is shown in Figure 1. The electric charge induced on a sensing electrode can be calculated based on equations (1) – (3). Equations show that charge q, inducted in time moment t is proportional to electric field strength E and effective exposed area of the sensing electrode [16].

$$\oint_S E dS = \frac{Q}{\epsilon} \tag{1}$$

$$q\left(t\right) = E_{\epsilon_0} s\left(t\right) \tag{2}$$

$$i\left(t\right) = E\frac{\partial s\left(t\right)}{\epsilon_0 \partial t} \tag{3}$$

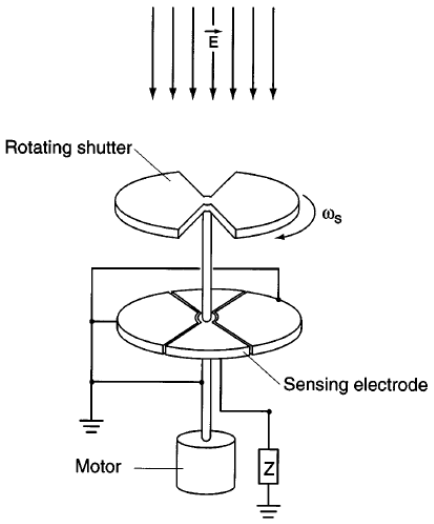

Fig. 1: Field mill for measurement of the polarity and magnitude of an electrostatic field [16].

Where:
E — electric field strength
$i\left(t\right)$ — current inducted on the sensing electrode
ϵ_0 — electric permittivity of free space
$s\left(t\right)$ — exposed area of the sensing electrode

An exposed area of the sensing electrode for constant angular velocity creates a triangular wave function. Derivation of the triangle function generates a square wave of the current. Amplitude of that current is equal to:

$$I = \frac{\omega}{\pi}\epsilon_0 S E \tag{4}$$

Where:
I — square wave current amplitude
ω — mill angular velocity
S — sensing electrode area

The above presented equation allows to calculate the maximum current generated for a defined E. What is more, it shows that the generated current is dependent from the angular velocity of the modulator. So, to eliminate this effect, the modulator angular velocity should be stabilized at a constant level.

A sensor prototype was designed and assembled, based on the discussed theoretical assumptions. The technical solution (size, weight, energy consumption, method of communication) has been selected in terms of the possibility of installation on the drone. It contains several components which are critical for the entire system operation. The heart of the sensor is a 32bit Cortex-M4F microcontroller with 16bit differential input and analog to digital converter (ADC). The microcontroller controls the modulator propeller by the DC motor via a half-bridge power source. To provide information about angular velocity, an encoder was applied. The propeller is modulating constant electric field and this way generates charge at the detector. In the next step, the charge is amplified by an analog

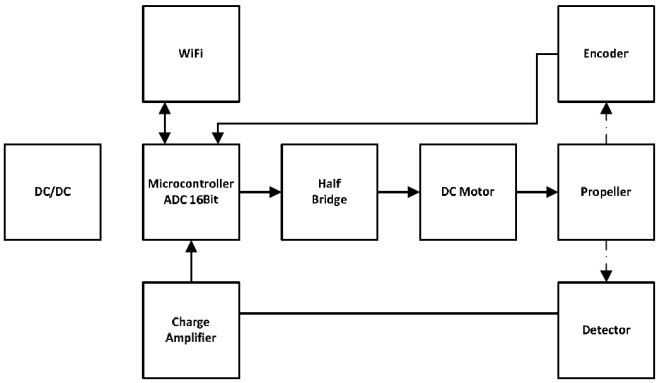

Fig. 2: Sensor block diagram.

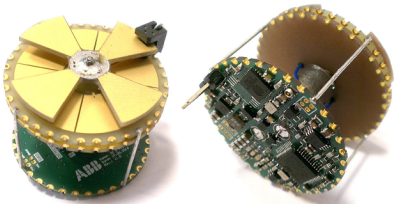

Fig. 3: Entire device assembled picture. Rotating part with encoder and electronic controller are visible, with miniature electric motor in between.

circuit. The signal from the charge amplifier is connected to the microcontroller and the ADC constantly measures the input signal. The microcontroller is processing the collected data and is able to transfer it to a smartphone or PC application via a Wi-Fi connection. The entire system is powered by a DC/DC converter. The block diagram of the proposed system is presented in Figure 2, whereas the DC field sensor is shown in Figure 3.

An AC field sensor with a very similar but simplified design was also developed. The sensors have been checked and calibrated in a known electric field, for linearity and high measurement accuracy. Characteristics have been determined and hence the error rate is less than 5 percent over the entire measuring range.

III. Experiments with AC and DC field measurement

The developed AC and DC field sensors were tested in real conditions. The first test was made with a statically electrified poly-carbon plate. The second one was done in a well controlled condition, using a high voltage DC generator connected to a flat metal plate. Also a test with high voltage power lines was done. This enabled to check the effectiveness of the sensors mounted at the drone, and also to indicate possible directions in the development of the measurement platform. It was important to check how easy it was to make measurements, as well as what methods of flight support and automation could be used.

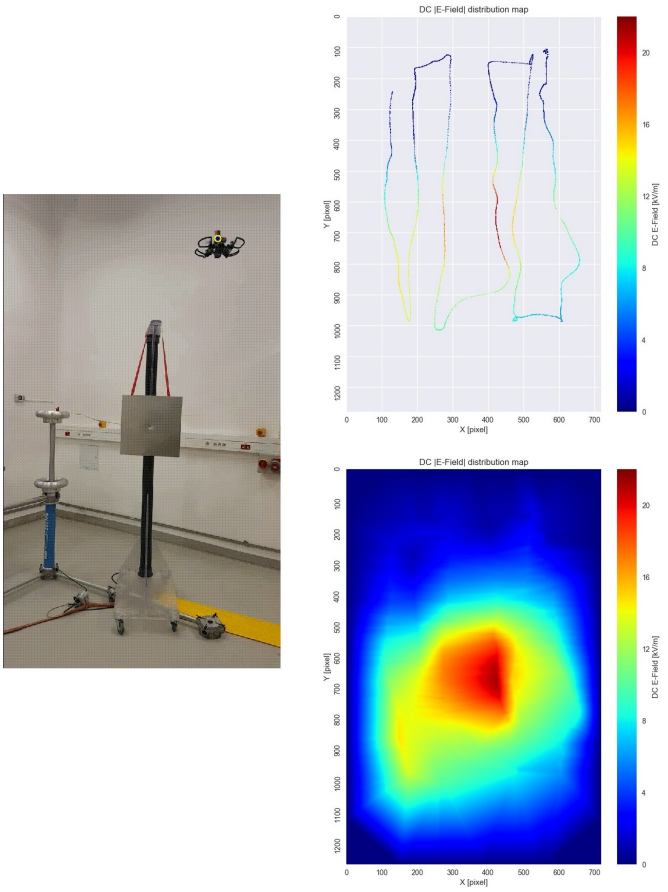

Fig. 4: A charged plate and the drone with the DC field sensor. The left figure presents the measurement object, the middle shows the track of recorded drone position with the field amplitude, and the right figure presents the extrapolated field distribution in the visible area based on the measurements. Shape of the plate is clearly visible in the field distribution.

Figure 4 shows an experiment where the drone was flying in front of an electrified metal plate with a DC field sensor. The drone was manually controlled and its position visually tracked. During the flight, careful observation by a human was needed to keep the drone in a constant distance from the measured object. At the same time a camera was employed to record position of the drone in horizontal and vertical directions. The recorded measurements, presented in the middle plot in Figure 4, show how difficult it is to measure the field using manual control of the drone. In result, the use of interpolation then becomes necessary, but it brings an inevitable loss of precision.

Figure 5 shows the flying near the 110 kV AC high voltage line. The drone, as before for the DC field mapping, was manually controlled, and its position was tracked based on GPS information. The measurements were visualized, as shown in Figure 6.

The performed experiments revealed that the development of an autonomous platform enabling measurements with mini-

Fig. 5: Drone path view (green) under power line. A high voltage electric pole is visible in the right-top corner.

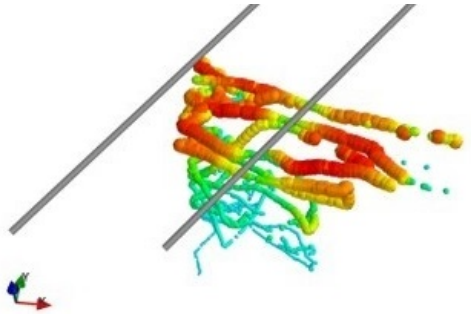

Fig. 6: AC field measurement visualization under a 110 kV power line. The bigger and redder dots mean stronger field.

mal operator intervention is a necessity. In the considered case, measurements repeatability is extremely important and it can be obtained among others by flying along the same trajectories. Thanks to this, it will be possible to perform for example periodic inspection with improved control over measurements.

IV. The Proposed Vision-Based System

The authors have built a system based on visual feedback that enables autonomous flights of the drone with an electric field sensor installed on its body.

In the discussed system, the autonomous control structure shown in Figure 7 was proposed. The drone's flight is observed by a single fixed camera, capturing the entire area available to the drone in the current flight. Moving an energy-consuming element such as a computing unit to a stationary position with its own power supply does not limit the flight autonomy in any way. The drone itself is powered by batteries. The same battery is used to power the electric field sensor together with its communication module, however the energy consumption of this module is small compared to the consumption by the drone for the flight. The battery capacity limits the flight autonomy to several minutes, which in practice, however, is enough to perform even quite complex scans.

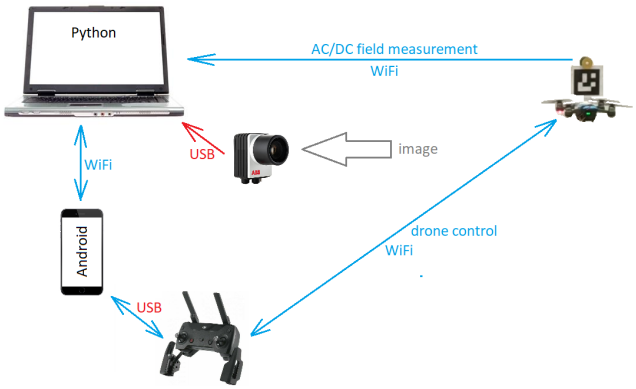

Fig. 7: Proposed system for high-voltage field measurement.

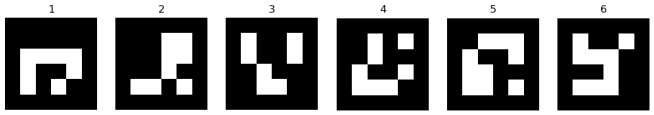

Fig. 8: ArUco 4x4 markers with numbers from 1 to 6.

Increasing the drone flight time could be achieved by increasing the battery capacity. It is possible, however, only within certain boundaries limited by the drone's payload. In general, it would be necessary to use a larger drone, with a higher payload, with a more favorable factor determining the possible flight autonomy.

The ArUco markers (and its implementation from the OpenCV library) were used to locate characteristic points [17]. They are a kind of 2D code consisting of white and black boxes (Fig. 8). Each marker encodes one number and, by definition, is a square of a given size. Knowing the dimensions of the marker and the internal parameters of the camera, it is possible to convert between the camera coordinates and the marker coordinates. As a result, with one camera, the full information about the position and orientation of the marker is available. Therefore, in a common global coordinate system, the camera, the ArUco markers and the calculated drone 3D position are placed. Also, coordinates in the Cartesian space can be expressed in real units such as centimeters. The detection and orientation estimation of ArUco markers are possible with the use of dedicated functions provided in the OpenCV library. Furthermore, a number of additional functions for geometric transformations and calculation of trajectories in three-dimensional space have been written.

In the proposed system, the ArUco markers were used for two purposes. The first one was to define the flight trajectory. For this purpose, four markers with known identifiers were placed on one plane. Three of these markers identified the plane, and the fourth was used to more precisely define the dimensions of the rectangle. The plane determined in this way served as the basis for defining the scanning trajectory. Various

scenarios of determining the trajectory and different types of it are also possible, for example cylindrical or linear. It all depends on the specific application. An example of ArUco markers placed on the wall is shown in Figure 9. In the same picture also the source of the electric field is visible.

The control software allows selection the number of scan planes, the distance from the base plane, the distance between the planes, the distance between the lines of successive flights, and other parameters that determine the geometric location of successive lines of flight. Importantly, the base plane scan is only required once. This is due to the fact that the position of the camera is constant and unchanging, and the single determination of the base plane invariably links the coordinate system of the scanned space with the camera coordinate system.

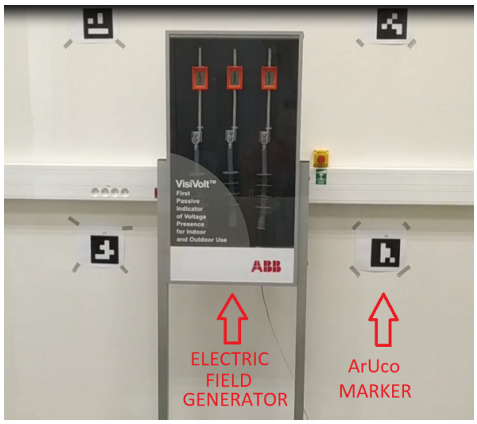

Fig. 9: ArUco markers placed on the wall used for base surface detection.

A real example of four surfaces with trajectories, is presented in Figure 10. The drawing shows the base surface determined on the basis of markers. In front of it, four planes with horizontal lines representing the drone's lines of flight (trajectories) are visible. The number of planes, the spacing of lines within a plane, and the distance between scan points are fully configurable. Values can be entered in centimeters. In the same 3D space also the camera position is shown.

The second purpose of using the ArUco marker is tracking the position and orientation of the drone. The aerial vehicle is equipped with a marker mounted on a special arm. Its size may, of course, differ from the markers used to define the base plane and therefore be better adapted to the size of the drone and the distance from the camera. The marker on the drone is used to obtain the current position and orientation of the drone in relation to the trajectory, based on its size and shape (Fig. 11). To achieve good results, the camera must be previously calibrated to be sure, that all aberrations are corrected.

V. Control

The drone control is centralized. The system, shown in Figure 7, used a control system presented in Figure 12. The position of the drone is determined on the basis of the image registered by a stationary camera, which is observing the

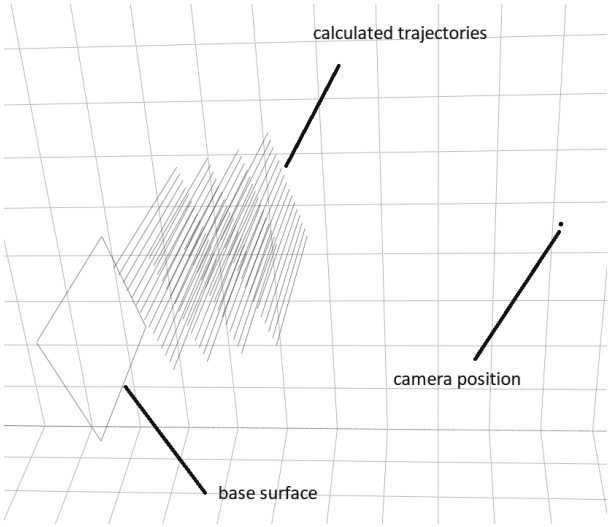

Fig. 10: Measured base surface (initial scan), calculated trajectories and camera position, based on single camera image.

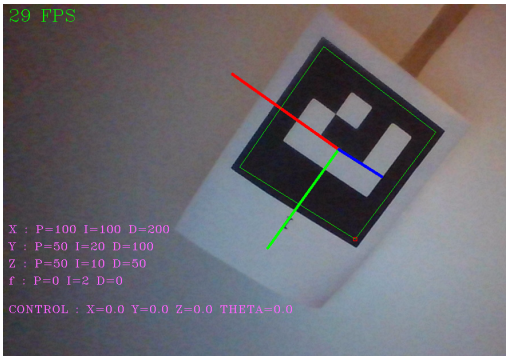

Fig. 11: Single ArUco marker with calculated vectors.

ArUco marker mounted on the drone. The set position for the x, y and z coordinates is calculated on the basis of successively calculated points lying on the trajectory. The positioning error in the x, y and z coordinates and for the rotation around the vertical axis of the drone (yaw) serves as the input for four PID regulators. The other two rotations of the drone (pan, tilt) are stabilized by the drone's internal, independent mechanisms. This is expected, as the flight mechanics of a quad-copter drone involves pan and tilts during forward and sideways flight. Thus, stabilizing the rotation about these axes has no justification, and even is not possible. The parameters of the PID controllers were selected in accordance with the Ziegler-Nichols methodology.

Physically, the system of regulators, as well as the entire image processing path, has been implemented on a PC computer in Python. The output control values for the four degrees of freedom (x, y, z, yaw) were sent via the Wi-Fi network to the gateway (in the form of an Android device) present in the same network. A specially created application was run on this device. Its task was to translate the protocols between the controls generated by PID regulators and the commands

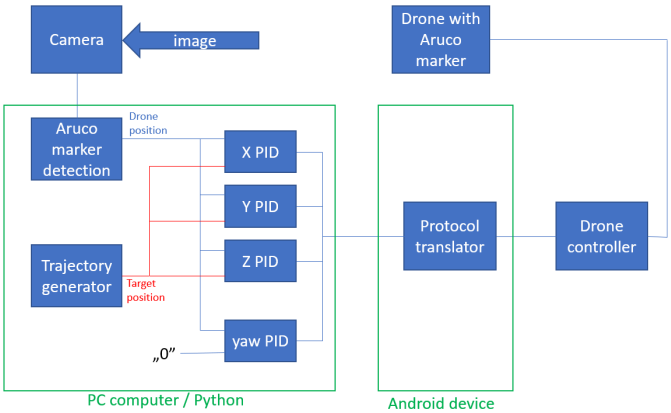

Fig. 12: Control block diagram.

understood by the drone's API. The application was connected via Wi-Fi directly to the drone. The feedback loop was closed by changing the drone's position in response to control from the regulators, which was recorded by a camera connected to the computer running the control program.

VI. Experiments

Figure 13 shows photos of the drone with the three developed sensors. Those sensors were tested in different environments and scenarios. The pictures present a) the DC field sensor b) the AC field sensor and c) the omnidirectional AC field sensor, all installed on top of the drone. The sensor could be easy replaceable with another.

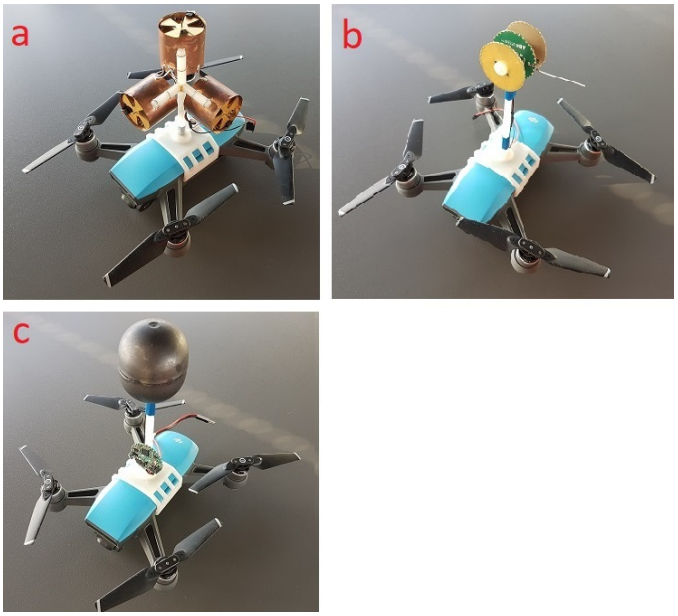

Fig. 13: Drone with 3 types of evaluated electric field sensors: DC 3-axes (a), AC 1-axis (b), Omnidirectional AC (c)

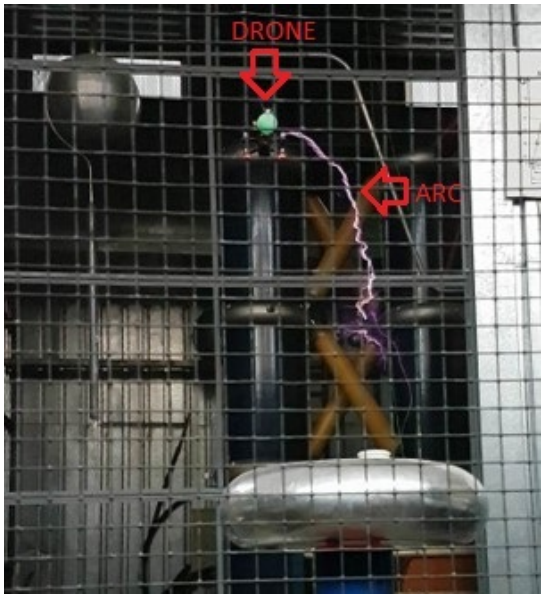

Fig. 14: Arc from Tesla coil is "touching" the drone.

A. Close contact with high voltage

The resistance of the drone with the installed sensor to the direct impact of electric discharges was experimentally tested. Figure 14 shows the flight of the drone near a Tesla coil, generating discharges with a voltage of around 1 million V. It can be seen that the arc "touched" the drone. However, this did not have a negative impact on the drone itself, as well as on the field sensors mounted on it, apart from exceeding the reading ranges during the electric arc appearance. This resistance comes directly from the fact that the drone is isolated from the ground potential.

B. Fully autonomous flight

The proposed system, although in an experimental phase, ensured a high degree of work automation, and therefore the possibility of practical application. It requires one preparatory step, namely scanning the base plane. The results of this scan are stored in a file, so there is no need to repeat the procedure before every measurement. Of course, the camera must be calibrated beforehand, which means determining its internal parameters (transformation and rotation matrix). Then, it is enough to define the trajectories by specifying the number of scanning planes, the distance from the base plane, the distance between the planes, and the density of the points grid. The next step is to command the drone to take off. From now on, the drone follows the preset trajectory, scans the electric field, transmits the results from the sensor, and after completing the work, it automatically lands in the place from which it took off.

Figure 15 shows such a fully automatic drone flight in front of a device generating an AC electric field. In the presented example, the drone scanned the trajectories located on one plane, which was determined on the basis of markers previously stuck onto the wall. The image is divided into two

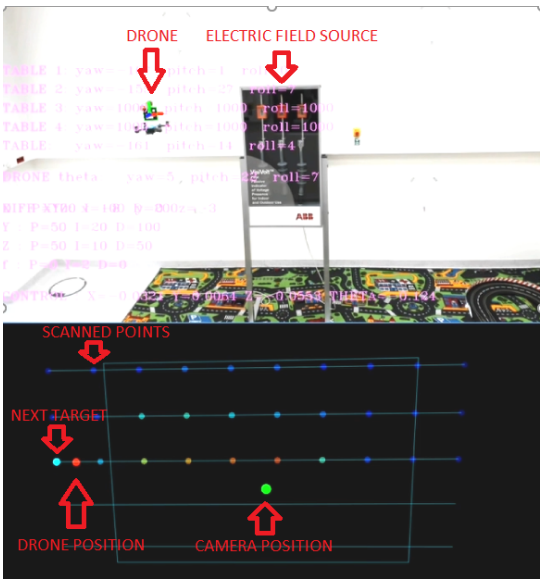

Fig. 15: Drone during autonomous flight. The source of the electric field is visible in the center. The drone is flying in front of that source and is scanning the electric field.

parts. The upper part shows a frame from the camera. The board in the middle is used to generate an electric field. The drone, visible on the left-hand side, is equipped with an AC field sensor and an ArUco marker. In the lower part one can see the currently generated scan image. The green dot in the center of the image represents the position of the camera. The red dot represents the current position of the drone. In turn, the colored dots – from dark blue to orange – represent the values of the electric field at fixed points in the spaces lying on the already scanned trace. During the flight of the drone, the values of the electric field, continuously measured by the sensor, were sampled at the moments in which the drone reached the target positions in the network nodes. The read values produced a sparse field density map.

Measurement map resolution and more precisely the density of measurement points is limited by optical factors: the resolution of the image recorded by the camera and the distance between the drone and the camera. The lower camera resolution or the greater distance between the drone and the camera results in a smaller ArUco marker in the image. Below a certain limit it is not continuously detected and the visual feedback loop is terminated. On the other hand, the computing power limits the resolution of the processed frame, because the effectiveness of the drone position control requires in practice at least a dozen or so frames per second.

Different camera resolutions were tested to determine maximum data throughput for on-line operation of the system. The summary is presented in Table I. For control purposes it was concluded that minimum 20 fps is required. That camera speed with the used hardware allowed us to use the highest resolution of 1080x720 pixels what was sufficient for operating the system. Higher resolutions causes significant drop of fps. These

TABLE I: Performance

Item	Best value	Reference
Resolution	1080x720	1920x1080
Frames per second *	20	6

*i7-2720QM(2.2GHz), 4 GB RAM, 2GB Nvidia Quadro 1000M

TABLE II: Example setup of tracking parameters

Item	Value
Distance camera-drone	2-3 m
Distance camera-wall	5 cm
Horizontal grid	10 cm
Vertical grid	10 cm
Depth grid	20 cm
Drone ArUco size	74 x 74 mm
Wall ArUco size	245 x 245 mm

values are optimal for the computer that was used for testing. However, they can be larger, provided that a faster computer is used and multi-threading is implemented, preferably with the use of a GPU. Table II shows the parameters that turned out to be the best for the selected camera resolution, ensuring a smooth flight of the drone. Those parameters determine serviceable distance from the camera, trajectories geometry and preferable ArUco markers sizes.

The mentioned optical parameters and the resulting image processing performance affect the achievable scanning speeds. The adjustment between the parameters of the PID regulators controlling the flight speed of the drone and the gap between the target (scanning) points also has a very significant impact on this speed. The smaller distance between the points, i.e. the denser mesh, the slower and more precise the flight is required. On the other hand, the scattered mesh, the faster flight of the drone can be. In every case proper tuning of the controls is required to avoid oscillations in reaching the next target positions. For example, for the one-plane trajectory presented in the figure 15 with a distance between points equal to 10 x 10 cm and the total number of such points equal to 70, the scanning time, including the automatic take-off and automatic landing in the same place from which the site took off, was two minutes.

In order to better illustrate the field distribution, a measurement visualization is also proposed. That step takes advantage of the information available from the measurement trajectory setting. Thus, the initial information is the size of the plane as well as the number of points in horizontal and vertical directions per each plane. Based on all the values measured in the specified nodes, an interpolation is performed. For that task the Smooth Bivariate Spline [18] is selected, as that method allows for good preservation of spline interpolation on a 2 dimensional plane. In the next step, a mesh grid of higher density is generated and the interpolation function is evaluated on the additionally generated nodes. For the presented case that grid is 100 times more dense than the measured nodes. An example of the measurement visualization result is presented in Figure 16.

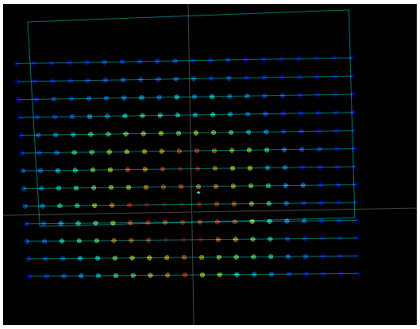

(a) Measured field on the specified grid depicted by colour of markers.

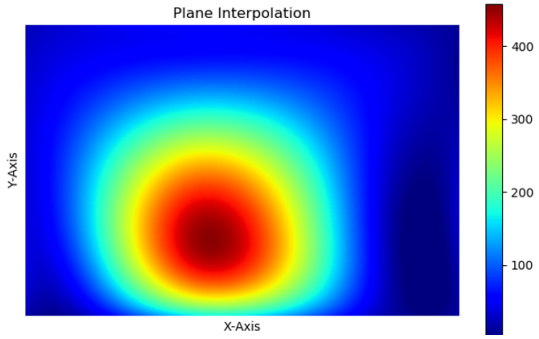

(b) Interpolated field distribution for the specified plane.

Fig. 16: Measured points (a) and visualization of full area after interpolation (b).

VII. Summary

In this paper a comprehensive description of a fully autonomous drone for electric field scanning was presented. The work covers numerous aspects of that complex system, namely:

- electric field sensor description for both AC and DC measurement,
- evaluation of field sensors performance in various conditions, from laboratory to field experiment,
- vision based control system, using ArUco markers, able to identify the drone position and area of operation,
- centralized control algorithm enabling mission planning.

The proposed system effectively presents the possibilities of using drones to measure electrical quantities in a harsh environment, such as the immediate vicinity of devices operating at very high voltage. This approach is safe for the stuff, as a drone can get much closer to the tested devices without any special security measures. Automatic control enables initial metering of objects (such as switchboards, radio masts) in order to collect information about their geometry (exactly like described base surface), and then regularly, easily, the quick scan of the considered space. The operator's participation is limited to issuing a start command and the scanning process itself is fully autonomous, following repetitive trajectories.

It is possible to use such a system for early detection of field anomalies caused by e.g. shielding, grounding or insulation damage. The proposed solution can work well in periodic condition monitoring – it could be used in a scenario of flying the same scan path every certain time (e.g. weekly, monthly) and comparing the results while the device is running. Progressive discrepancies visible for comparable working conditions may be a clear signal of a possible damage. As a result, a fault can be detected even before its consequences begin to be noticed, in line with the predictive maintenance idea.

The presented system can be developed in the next steps. The most desirable option is to become independent from the use of ArUco markers for initial marking the scanned object. For this purpose, other methods of 3D scanning could be used, allowing for modeling the object (e.g. a transformer) and on this basis determining the trajectory in its vicinity. Another direction is the use of a faster computing platform based on, for example, GPU, which would allow the use of a camera with higher resolution. As a result, the accuracy of the drone's positioning and its allowable distance from the camera would be increased.

References

[1] K. Schon, "High Voltage Measurement Techniques, Fundamentals, Measuring Instruments, and Measuring Methods", 2019.

[2] Wenbin Zhang, Youhuan Ning, Chunguang Suo, "A Method Based on Multi-Sensor Data Fusion for UAV Safety Distance Diagnosis", 2019.

[3] W. Joseph, S. Aerts, M. Vandenbossche, A. Thielens, L. Martens, "Drone based mesurement system for radiofrequency exposure assesssment", Department of Information Technology, Ghent University/iMinds, 2017.

[4] Percepto, "Autonomous Drone-In-A-Box", https://percepto.co/solutions/ , last accessed = Sep 29, 2020,

[5] Hsiu-Min Chuang, Dongqing He, Akio Namiki, "Autonomous Target Tracking of UAV Using High-Speed Visual Feedback", Applied Sciences, 2019.

[6] Young-Hoon Jin, Kwang-Woo Ko, Won-Hyung Lee, "An Indoor Location-Based Positioning System Using Stereo Vision with the Drone Camera", Location-Based Mobile Marketing Innovations, 2018.

[7] R. Opromolla, G. Fasano, G. Rufino, M. Grassi and A. Savvaris, "LIDAR-inertial integration for UAV localization and mapping in complex environments," 2016 International Conference on Unmanned Aircraft Systems (ICUAS), 2016, pp. 649-656, doi: 10.1109/ICUAS.2016.7502580.

[8] J. Delmerico, D. Scaramuzza, "A Benchmark Comparison of Monocular Visual-Inertial Odometry Algorithms for Flying Robots", 2018.

[9] DragonFly, "Precise 3D location for robots, drones, AGV and Forklifts using standard cameras and SLAM", https://dragonflycv.com, last accessed Sep 29, 2020

[10] J. Flynt, "GCP vs RTK vs PPK Aerial Mapping: Which is Better?" https://3dinsider.com/gcp-vs-rtk-vs-ppk/ , 2019.

[11] H. Kinjo, M. Morita, S. Sato, T. Suriyon and T. Anezaki, "Infrastructure (transmission line) check autonomous flight drone (1)," 2017 International Conference on Intelligent Informatics and Biomedical Sciences (ICIIBMS), 2017, pp. 206-209, doi: 10.1109/ICIIBMS.2017.8279694.

[12] A. Hatibovic and P. Kádár, "The application of autonomous drones in the environment of overhead lines," 2018 IEEE 18th International Symposium on Computational Intelligence and Informatics (CINTI), 2018, pp. 000289-00294, doi: 10.1109/CINTI.2018.8928234.

[13] International Micro Air Vehicles, Conferences and Competitions, http://www.imavs.org, last accessed 2021.

[14] R. Miles, T. Bond, G. Meyer, "Report on Non-Contact DC",Lawrence Livermore National Laboratory, 2009.

[15] J. S. Shafran, "A MEMS-Based, High-Resolution Electric-Field Meter", Masters Thesis MIT, 2005.

[16] M. K. David A. Hill, "Electric Field Strength", 1999.

[17] Open Source Computer Vision: ArUco Marker Detection for Python, https://docs.opencv.org/master/d9/d6a/group__aruco.html, last accessed 2020.

[18] Open source scientific tools for Python – Smooth Bivariate Spline, https://docs.scipy.org/doc/scipy/reference/generated/scipy.interpolate.SmoothBivariateSpline.html, last accessed 2020.